C. R. Physique 15 (2014) 674–682

Contents lists available at ScienceDirect

Comptes Rendus Physique

www.sciencedirect.com

Liquid and solid foams / Mousses liquides et solides

Structural characterization of solid foams

Caractérisation structurale des mousses solides

Éric Maire *, Jérôme Adrien, Clémence Petit

INSA de Lyon, MATEIS CNRS UMR5510, Université de Lyon, 69621 Villeurbanne, France

ARTICLE INFO

Article history:
Available online 26 September 2014

Keywords:
X-ray tomography
Cellular materials
Image analysis
SEM
3D

Mots-clés :
Tomographie aux rayons X
Matériaux cellulaires
Analyse d'images
MEB
3D

ABSTRACT

For being a useful contribution to the understanding of the properties of solid foams, the characterization of the structure of solid foams has to be performed at different scales. The microstructure of the solid part of the foams has to be analyzed. For this, standard SEM observations are often used. The most important aspect (and the most problematic) remains the characterization of the porous architecture of these materials. The methods introduced in this paper concern both scales and the article discusses the specificity of the experiments in the case of porous materials. X-ray tomography is described in more details because it becomes widely used for this purpose. The paper also shows how the obtained 3D images (sometimes obtained during deformation) can be processed to yield important morphological parameters describing the foams.

RÉSUMÉ

Pour être utile à la compréhension des propriétés des mousses solides, la caractérisation de la microstructure de ces mousses doit s'effectuer à différentes échelles. La microstructure du matériau constituant la phase solide doit être connue. Pour ceci, le MEB est le plus souvent utilisé. L'aspect le plus important (et le plus problématique) est la caractérisation de l'architecture poreuse de ces matériaux. Les méthodes de caractérisation présentées dans cet article concernent ces deux types de caractérisations et les spécificités expérimentales liées à la nature poreuse des échantillons. La tomographie aux rayons X est décrite plus en détail, car c'est la méthode la plus utilisée. L'article montre aussi comment les images 3D obtenues, y compris en cours de déformation, sont traitées pour obtenir les paramètres décrivant la morphologie poreuse des mousses solides.

1. Introduction

Solid Foams (SF), the subject of a part of this thematic issue, are open- or closed-cell foams, having their solid part made of metal, ceramic, or polymer. They form a widely expanding new category of materials available for engineers. Polymer foams have been used for many years in the packaging industry, at a large industrial scale, for thermal insulation of buildings or for comfort applications (seats etc.). Ceramic foams are employed as high temperature filters and gas burners in

* Corresponding author.

http://dx.doi.org/10.1016/j.crhy.2014.09.001
1631-0705/

several devices or processes for many years as well. The most recent family of these materials is that of metallic foams, the properties of which have been reviewed and presented in [1,2]. The possibility of using these materials for new applications has drawn a lot of attention on the family of SFs in the recent years.

The literature on this category of materials is now relatively rich. The book *Cellular Solids* by Gibson and Ashby [3] provides for instance a broad survey of the understanding of the mechanical behavior of a wide range of SFs. It is apparent in this literature that for a good analysis of the macroscopic properties of this type of materials, two scales of microstructure have to be distinguished and analyzed:

- the microstructure of the solid part of the material, at various scales,
- the cellular microstructure also referred to in recent studies as the "architecture" of the SF.

The microstructure of the solid phase in a SF is important to characterize, because most of the time, it differs from its counterpart in the equivalent bulk material. Relying on published and tabulated values of the properties of the bulk solid can then lead to important mistakes. The analysis of this microstructure in terms of inclusions, pores, precipitates, grains, dislocations is very similar to the standard analysis of the bulk equivalent. There will be no description in this paper of all the different techniques available to characterize the solid part at different scales, because this is a rather straightforward conventional discipline generally referred to as "microscopy". In the first part of this paper, we will then give brief examples of the peculiarity of the microstructure of the solid part of SFs, with no emphasis on the technique.

As already mentioned, the architecture will be the term used in the present paper to designate the morphology of the arrangement of the solid and gaseous phases. This has a first-order importance on the properties and has then to be characterized in details. All the crucial morphological parameters (such as orientation, size, shape of each cell) are important to measure for a correct quantification of the cellular microstructure. Ideally, these measurements should be performed on a three-dimensional image of the sample. The second part of this paper will then describe the methods available to obtain a 3D image of a sample at various scales. X-Ray Computed Tomography (XRCT) has appeared in the last two decades to be a very powerful tool allowing one to characterize the architecture of SFs [4–12]. It is nowadays a versatile technique capable of providing non-destructive three-dimensional images of a SF. Some of the most important studies of the architecture of solid foams using X-ray tomography are reviewed in the third part of this paper. In the fourth part, it will be shown how the tomographic images can be used quantitatively to extract key parameters for the cellular microstructure. In the final fifth part, we will give examples of deformation modes studied using dedicated experimental loading rigs.

2. 2D microscopy of solid foams

2.1. SEM observation of the structure

The complex 3D architecture of solid foams requires observation techniques permitting a high depth of field. Amongst the standard available techniques, only SEM shows enough depth of focus to apprehend the structure of these materials. SEM is then commonly used, with a moderate resolution, to measure apparent strut or wall thickness, pore size, etc. Any paper dealing with the characterization of solid foams usually uses SEM to describe the material qualitatively, and many examples can be found in the literature. For illustration purposes, we give in Fig. 1 a visual example obtained on a Fe–Cr foam processed by de-alloying in a molten metallic bath [13]. Note for example a work [14] where the resolution power of the SEM is used to observe nanoporous metal foams. In terms of quantification, SEM can also be used to measure some parameters. The size of the walls or struts can be measured like in the case of nanoporous gold in [15], but one has to be careful not to overestimate the dimensions and to quote these as "apparent" sizes. The size of the windows connecting two pores is often an important morphological parameter to measure [16]. This can be derived reasonably well using SEM with a little bit of tilting if necessary.

Standard SEM is systematically used for ceramic foams. In [17] and [18], EDX has been used to analyze the composition of the foam after fabrication. Although more sensitive to electron irradiation damage, polymer foams have also been studied by SEM for example in [19] where the morphology of the porous network is visualized after cryofracture to obtain a nice and clean surface.

SEM is commonly used to observe the fracture surface of materials. It applies also for solid foams and has been used to help understand the fracture process. In [20], the fracture process of a metal hollow sphere structure in tension fatigue is elucidated using the morphological analysis with SEM. In Goussery et al. [21], the creep and high-temperature deformation behavior is also studied using this method on nickel foams. In [22], this is used to analyze the mechanical properties of replicated Al foams in creep and fatigue. In [23], this is achieved for analyzing the fatigue fracture surface of ERG aluminum foams.

2.2. Polished sections

Standard microscopy techniques can be used to analyze the microstructure of solid foams on polished sections. To achieve this normally simple and rather standard observation, in the special case of solid foams, there are a number of experimental difficulties related to sample preparation. If the fraction of solid is small, the foam is sometimes too weak to be correctly

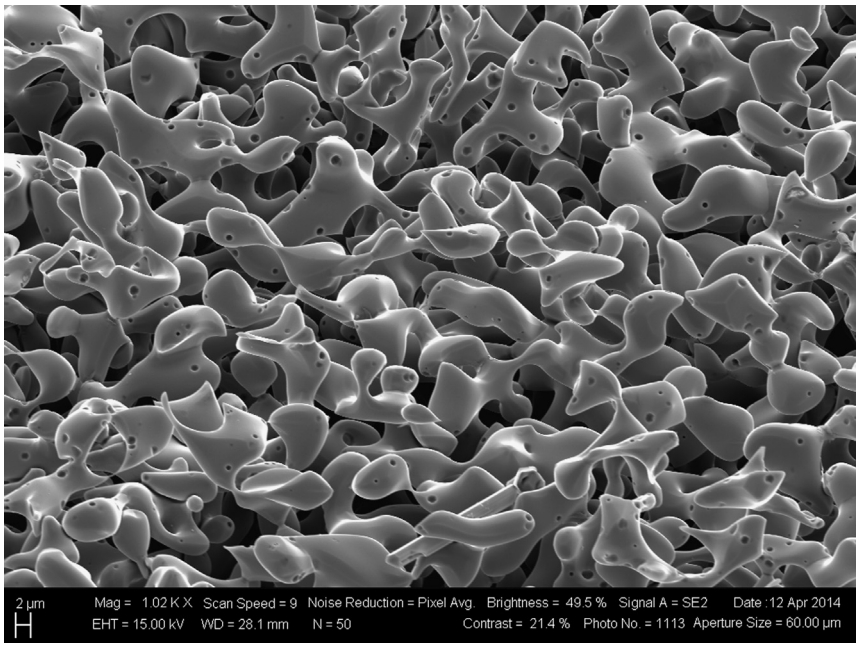

Fig. 1. SEM micrograph of a Fe–Cr metallic foam obtained by de-alloying an initial FeCrNi homogeneous precursor into a molten Mg bath.

polished, the struts and the walls bending or breaking during the polishing step. The gaseous part of the solid foams has in this case to be filled with some molding resin (plaster has also been used in some occasions). The sample being so prepared, it is then possible to polish the surface and analyze the microstructure of the solid part in terms of grains, inclusions, etc. In some cases, the cellular structure is strong enough to be polished without molding [24].

The aim of these studies of polished sections is generally to verify if the solid material in the foam is comparable to its equivalent in a bulk form. Quite often, it has been observed that it is not the case. An example can be seen in the paper by Gergely and Clyne [25] describing the microstructure of a metallic foam produced by the Formgrip^{TM} process. In this figure, it can be observed that the location of ceramic particles in the wall of a metallic foam is quite heterogeneous. Similar observations have been made on Duralcan MMCs. Using standard imaging and EDX, Amsterdam et al. have carefully studied the intermetallic content of ERG Al-based foams [26] in order to relate these to the fracture properties of the struts in a specially designed model of the fracture of foams. In [24], intermetallics are also observed in struts. This means that the mechanical behavior of the solid part in solid foams is probably very heterogeneous from one strut to its neighbor.

Note finally that if the section is polished, EBSD can be used. This has been the case in some instances in Ni foams [21,27] and aluminum foams [22]. In both cases, it was shown that very few grains are present along the thickness of walls or struts, leading again to a local behavior varying quite strongly from one strut to its neighbor.

3. General panorama of 3D imaging methods

Solid foams have a complex 3D architecture. Although this can be analyzed partly using SEM, as shown in the preceding section, a full 3D image is desirable to achieve the morphological characterization with no ambiguity.

Fig. 2 shows in a schematic way a general panorama of the methods available for obtaining three-dimensional images of a material. We classify these here in two categories: destructive and non-destructive methods. Destructive methods are based on the successive observation of the surface of the sample after sequential removal of layers of the material. The combination and stacking of these 2D slices lead to a 3D picture of the microstructure of the sample. Surface images are in general obtained by classical microscopy techniques (optical, electron, and more recently ion and atomic-force microscopy). Removing the layers can be achieved by mechanical, chemical, or electrochemical polishing or by ionic etching. Atom probe tomography can be somehow compared with the preceding methods. The material is imaged layer by layer, but the thickness between layers is of the scale of an interatomic distance. In each layer, the spatial resolution is also close to the atomic scale (a little bit less). The information obtained is then three-dimensional, but at the atomic scale.

Non-destructive methods are attractive as they allow one to study the evolution of the architecture or microstructure over time, a modality very much appreciated in materials science and engineering. All the non-destructive methods are based on the interaction between the sample and an electromagnetic beam of rays. Obtaining information about the microstructure without destroying the sample indeed requires probing it with a nondestructive ray. This ray must penetrate, interact and be transmitted out of the sample with an intensity sufficient to be collected and to convey information. Electrons (in the Transmission Electron Tomography—TEM—configuration), X-rays and neutrons (for radiography), acoustic waves

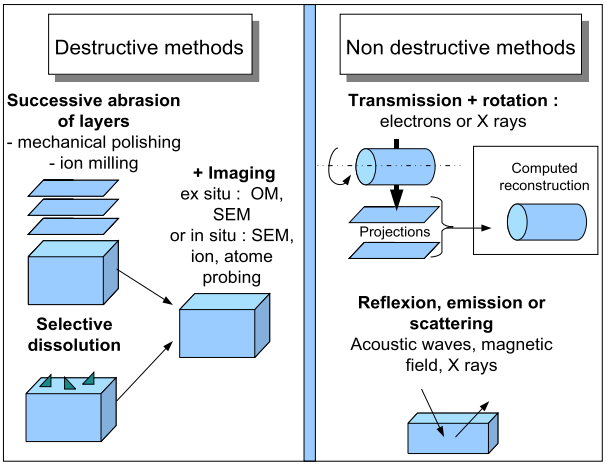

Fig. 2. General panorama of the methods available to obtain 3D images of a microstructure.

(scanning acoustic microscopy—SAM) or magnetic (Nuclear Magnetic Resonance—NMR) waves can alternatively be used for such probing.

Analyzing the depth of a sample is then achieved in two ways. If it is possible to focus the beam, then one can retrieve the reflected intensity from a given depth (this is the case in SAM). In this case, the sample can be raster scanned at different depths. The other way is to work in a transmission configuration using an appropriate detector (case of TEM, neutrons and X-ray radiography). The obtained projection contains information about the bulk of the sample. It becomes possible to deconvolve the projected signal by combining the information of a same region taken with different viewing angles, simply by rotating the sample between each acquisition. This reconstruction step of the 3D microstructure from two projections is computed. It was initially developed for X-rays for medical application in the 1970s and is constantly developing since then. The same reconstruction principle has been later applied to neutron and electron projections.

For solid foams, X-ray computed tomography has recently become widely used. It is non-destructive, able to access many different scales, the smallest being in the micrometer range. We will then focus on this method in the rest of the paper.

4. 3D Imaging of solid foams using X-ray tomography

4.1. Setups

The principle of projection/rotation explained in the preceding section is used here with X-rays, a very penetrating radiation for engineering materials. X-ray radiography for industrial applications has been used for many years for sample inspection. The experimental implementation of the X-ray tomography technique requires an X-ray source, a rotation stage, a radioscopic detector and a reconstruction software.

Two kinds of setups can be used for studying the cellular structure of solid foams:

- standard tomography can be performed using a laboratory X-ray source; several experimental setups are now commercially available and give good quality images with a resolution down to about 1 µm [28];
- a synchrotron source is required to perform high-resolution X-ray tomography [29]; this experiment can be performed on several beam lines at most of the existing synchrotron sources in the world today.

4.2. Qualitative results

For the characterization of the architecture of SF, the material can be considered as constituted of two phases (solid and gas), easily separated in XRCT because of their high difference in attenuation contrast. The acquisition of 3D images of this architecture by XRCT usually requires only a moderate resolution, as its typical size is often above 50 µm. Using a standard laboratory tomograph is then usually enough. Note however that more and more SFs appear with a nanoporous structure. This will be described later. The microscale is the scale of the microstructure of the solid part of the porous material. It can also be analyzed in 3D using XRCT with a higher magnification, as it will be shown in a subsequent paragraph. The resolution required is then sometimes below 1 µm.

4.2.1. Architecture

Fig. 3, extracted from one of our previous review [2], shows a selection of tomographic images of SFs. For an illustrative purpose, we have selected open- and closed-cell foams, the solid part of which are composed of metals, ceramics, or polymers. The mesostructure in all these materials is fluctuating and it appears important, for representativity reasons,

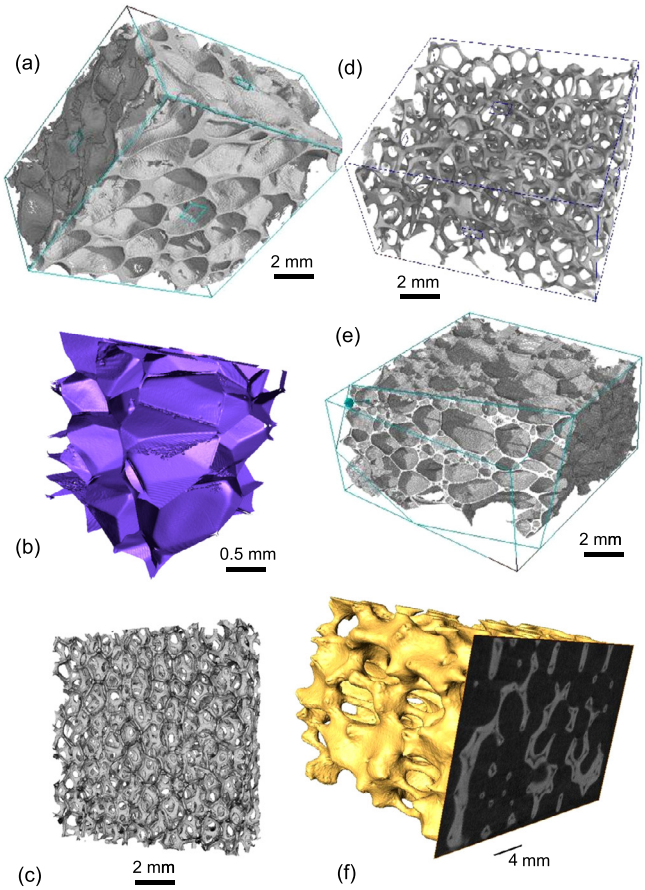

Fig. 3. (Color online.) From [2]. Various examples of the mesostructure of several SFs. (a) Aluminum closed-cell foam Alporas^{TM}. (b) A polymer closed-cell foam used for thermal insulation. (c) Nickel open-cell foam Nitech^{TM}. (d) Aluminum ERG^{TM} open-cell foam. (e) Aluminum closed-cell foam Formgrip^{TM}. (f) Al_2O_3 open-cell foam.

that the characterization of both the global properties and the mesostructure are performed on sufficiently large samples. A minimum of 10 cells across one lateral dimension can be used as a rule of thumb for estimating how large the sample should be. This implies that the magnification to be used to produce these images has to be quite low. In general, this precludes the simultaneous characterization of the microstructure inside the solid phase, as the resolution used to image the entire sample is too small to reveal the microstructure at a lower scale.

X-ray tomography is then versatile for qualitative visualization of the microstructure of solid foams. The technique is now widely used and what we said earlier about SEM also becomes true for X-ray tomography: there is hardly a paper dealing with these materials that do not include a 3D rendering of the architecture. The next sections present less frequent examples where the technique is used to visualize the microstructure at a smaller scale.

4.2.2. Microstructure and local tomography

The analysis of the microstructure of the solid phase in these highly porous materials is also an important part of the understanding of the properties. This can be achieved by increasing magnification, but this has long been thought to imply that the samples had to be cut in smaller pieces, to allow a good reconstruction in the tomography image. An example of the analysis of the microstructure inside an ERG single strut after appropriate cutting, using a resolution of 0.4 µm in our laboratory tomograph, is for instance shown in Fig. 4. The image is a slide reconstructed in the middle of a broken strut. The sample has been previously broken in tension and one can clearly see the multiple cracking of an intermetallic particle.

It has also been recently shown [30–33] that it was also possible to reconstruct a good quality image using the "local tomography"' concept in XRCT. Local tomography is achieved by scanning a sample larger than the field of view of the detector. This induces that some parts of the sample are not seen by the detector for some values of the rotation angle. Provided that this missing information induces only a weak perturbation (this is in particular the case for highly porous samples), the reconstruction can however be successful. Fig. 5 shows an example of reconstruction of an ERG^{TM} metal foam before fracture where we have performed tomography of a large sample (30×10 mm) using a rather high resolution (3 µm) leading to a lateral field of view of the detector of 5 mm only, i.e. much smaller than the size of the sample. This

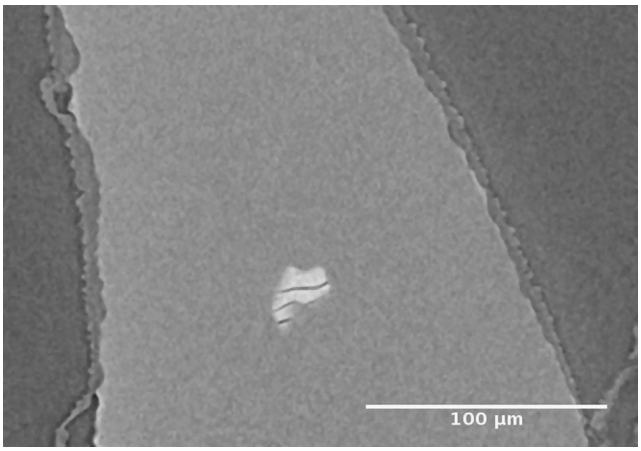

Fig. 4. Broken intermetallic particle in a strut of an ERG foam broken in tension. The tomogram was acquired with a 0.4-µm resolution using a tomograph designed by RX Solution.

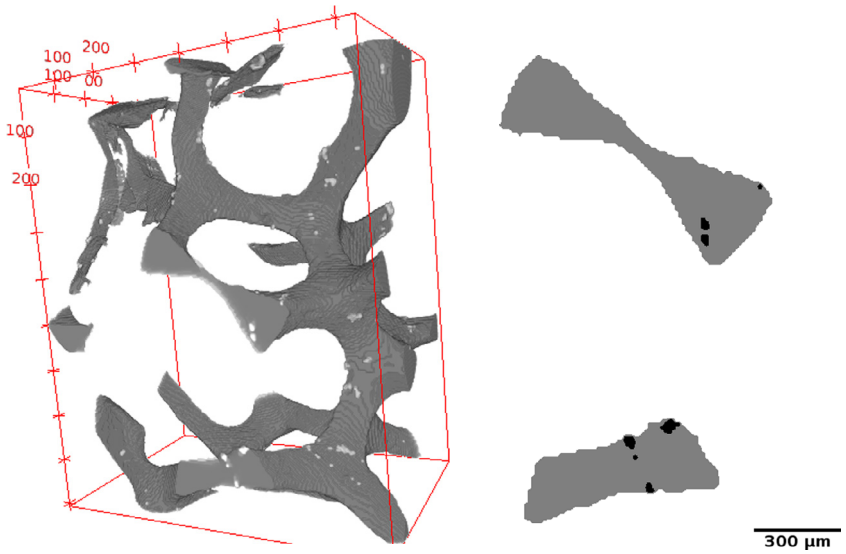

(a) (b)

Fig. 5. Local tomography visualization of inter-metallic particles inside an ERG foam. (a) Shows a 3D rendering and (b) a reconstructed tomographic slice. In (a) the particles are visible in white. They are black in (b).

was achieved without cutting the sample. The figure clearly shows the presence of fine inter-metallic particles and pores inside the solid phase, highlighting the capability to image fine details in large samples.

5. 3D image quantification

5.1. Density and size

The XRCT technique is even more powerful when used as a tool to quantify the architecture. The main important parameters required to characterize the architecture of a SF are: the global density and its fluctuation in the sample, the cell size distribution and the wall thickness distribution. We have, for instance, performed such a detailed characterization for several porous ceramics in [16] using selected samples containing pores of very different sizes. Because the tomographic data describes the three-dimensional structure, not only the global relative density of a sample could be measured, but also some density profiles calculated in slices as a function of the position of each slice could be easily created. This allowed us to assess the homogeneity of the distribution of the solid phase in the studied samples. We also characterized the size distribution of the pores and walls in this set of different materials using a now well-developed virtual granulometry technique based on sequential 3D image processing operations called “openings”. These operations were performed directly on the XRCT images and allowed us to measure the thickness distribution of the pores and of the walls. Olurin et al. [12] has

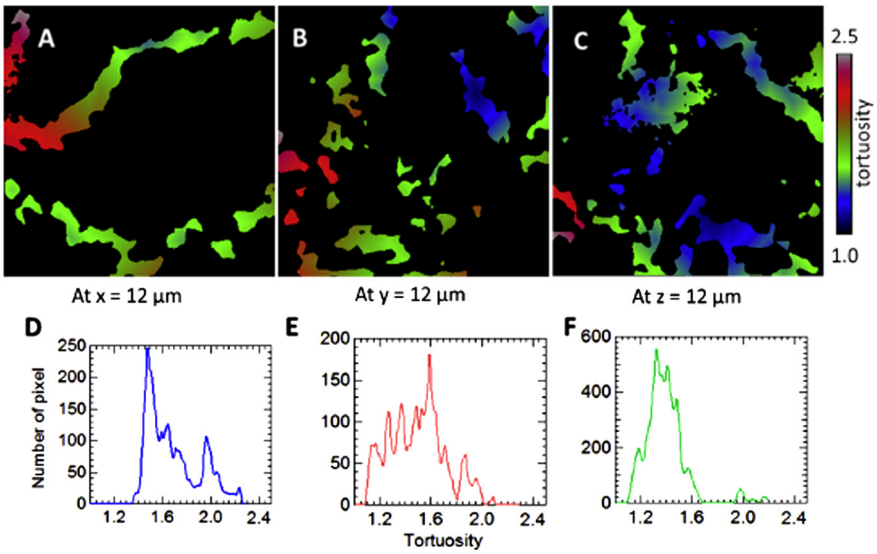

Fig. 6. (Color online.) From [34]. "Tortuosity distribution" of a $LiCoO_2$ sample shown as (A–C) spatial distribution maps and also (D–F) histograms for all three orthogonal directions along the positive direction.

also produced an important contribution to this field using the morphological parameters usually defined for bones and applying it to different kinds of metal foams. The paper includes a discussion of the effect on the results of the segmentation method and of the X-ray conditions (resolution, energy, integration time).

5.2. Other parameters

The information provided by X-ray tomography being fully three dimensional, post-processing with the purpose of separating open and closed porosity is possible. It is generally made by looking if one of the largest objects is touching the borders of the reconstructed volume. This object is then defined as the opened part of the porosity and the closed part can be analyzed separately by calculating the difference between the total porosity and the open porosity. The open part of the porosity is also often the largest of the pores and one can calculate the ratio of the volume of this largest pore over the total volume of porosity. This simple parameter is also called the connexity index.

One important parameter in describing the porous network in a given SF is its tortuosity, a measure of how direct the paths through the network are. Tortuosity can be measured using the 3D image of a SF using distance calculation. The different way of doing this has been summarized in [34]. Some examples of 3D visualization extracted from this paper are shown in Fig. 6. This parameter, very important in many applications, is rather difficult to measure using any other imaging technique.

For a tomographic reconstruction of a SF, it is rather easy to calculate the amount of surface between the solid and the gas present in the sample. This allows us to calculate the specific surface, of practical importance in the field of batteries. This was, for instance, achieved in [35].

The local radius of curvature is also sometimes a very useful parameter as it governs local melting (snow, solidification, [35,36]). It can be measured from the 3D shape of a surface-like structure shown in [37,38].

Finally, the size of the necks between two neighboring pores is an important parameter in scientific studies dealing with transport properties. Using dedicated watershed procedures, connected pores can be separated and the dimensions of the window between two pores measured [39].

6. *In-situ*/*ex-situ* experiments

To understand better the deformation modes of a material, it can be very useful to observe a same zone at different strain levels. However it is not trivial to apply an *in-situ* deformation during an XRCT experiment because the testing device has to rotate without screening the irradiation of the sample by the X-ray source. Special loading devices have been developed to allow such a rotation [7,28]. For tension or compression, a loading mode of interest for the present review, the forces between the top and the bottom grip are generally transmitted through an X-ray transparent tube surrounding the sample. In the case of metal foams, the main part of the deformation is permanent (plastic buckling and/or bending). It is then possible—and most of the time sufficient—to deform the SF outside of the tomograph, i.e. *ex situ*.

Using a furnace or coolers, it is also possible to induce *in situ* a change in a material by modifying temperature and to visualize the change using fast experiments. This has for instance been achieved to analyze the foaming process of metal solid foams [40,41]. In these cases, the changes in the microstructure were so quick that radiography was rather used

to analyze the dynamics of the process. The same procedure was also used with a cooling stage in [42] to analyze the fabrication of ceramic SF using the so-called "freeze casting" process. The dynamics was studied by radiography while the finally obtained architectures could be observed just after casting using tomography.

7. Conclusion

The structure of solid foams can be reasonably well characterized nowadays. SEM remains one of the best tools to both analyze the microstructure of the solid phase and also visualize the architecture and make some measurements of important morphological parameters. X-ray tomography appears now as another competitive versatile technique to achieve the same measurements with no ambiguity and at the two scales, the lower scale being accessible by cutting small samples or directly by local tomography. It also allows one to measure some inaccessible properties, such as specific surface and tortuosity.

Acknowledgements

Takeshi Wada, from IMR in Tohoku University Sendai Japan helped us to prepare the porous Fe–Cr alloy shown in Fig. 1 and to operate the SEM.

References

[1] L.J. Gibson, Mechanical behavior of metallic foams, Annu. Rev. Mater. Sci. 30 (2000) 191–227.
[2] É. Maire, X-ray tomography applied to the characterization of highly porous materials, Annu. Rev. Mater. Res. 42 (2012) 163–178.
[3] L.J. Gibson, M.F. Ashby, Cellular Solids: Structure and Properties, 2nd ed., Cambridge University Press, Cambridge, UK, 1997.
[4] H. Bart-Smith, A.F. Bastawros, D.R. Mumm, A.G. Evans, D.J. Sypeck, H.N.G. Wadley, Structure and mechanical properties of AFS sandwiches studied by in-situ compression tests in X-ray microtomography, Acta Mater. 46 (1998) 3582.
[5] E. Jasiuniene, J. Goebbels, B. Illerhaus, P. Lowe, A. Kottar, in: J. Banhart, M.F. Ashby, N.A. Fleck (Eds.), Cellular Metals and Metal Foaming Technology, Verlag MIT Publishing, 2001, p. 251.
[6] G. Gioux, T.M. McCormack, L.J. Gibson, Failure of aluminum foams under multiaxial loads, Int. J. Mech. Sci. 42 (2000) 1097–1117.
[7] B.K. Bay, T.S. Smith, D.P. Fyhrie, M. Saad, Digital volume correlation: three-dimensional strain mapping using X-ray tomography, Exp. Mech. 39 (3) (1999) 217–226.
[8] H.P. Degisher, A. Kottar, F. Foroughi, Determination of local mass density distribution, in: J. Baruchel, J.-Y. Buffière, É. Maire, P. Merle, G. Peix (Eds.), X-Ray Tomography in Material Science, Hermès Science, Paris, 2000, p. 165.
[9] A.H. Benouali, L. Froyen, in: J. Banhart, M. Ashby, N. Fleck (Eds.), Cellular Metals and Metal Foaming Technology, MIT-Verlag, Bremen, 2001, p. 269.
[10] A. Elmoutaouakkail, L. Salvo, É Maire, G. Peix, 2d and 3d characterisation of metal foams using X-ray tomography, Adv. Eng. Mater. 4 (2002) 803–807.
[11] L. Helfen, T. Baumbach, H. Stanzick, J. Banhart, A. Elmoutaouakkil, P. Cloetens, K. Schladitz, Viewing the early stage of metal foam formation by computed tomography using synchrotron radiation, Adv. Eng. Mater. 4 (2002) 808–813.
[12] O.B. Olurin, M. Arnold, C. Körner, R.F. Singer, The investigation of morphometric parameters of aluminium foams using micro-computed tomography, Mater. Sci. Eng. A 328 (2002) 334–343.
[13] Takeshi Wada, Kunio Yubuta, Akihisa Inoue, Hidemi Kato, Dealloying by metallic melt, Mater. Lett. 65 (7) (2011) 1076–1078.
[14] B.C. Tappan, S.A. Steiner III, E.P. Luther, Nanoporous metal foams, Angew. Chem., Int. Ed. 49 (2010) 4544–4565.
[15] A.M. Hodge, J.R. Hayes, J.A. Caro, J. Biener, A.V. Hamza, Characterization and mechanical behavior of nanoporous gold, Adv. Eng. Mater. 8 (9) (2006) 853–957.
[16] É Maire, P. Colombo, J. Adrien, L. Babout, L. Biasetto, Characterization of the morphology of cellular ceramics by 3D image processing of X-ray tomography data, J. Eur. Ceram. Soc. 27 (2007) 1973–1981.
[17] P. Colombo, T. Gambaryan-Roisman, M. Scheffler, P. Buhler, P. Greil, Conductive ceramic foams from preceramic polymers, J. Am. Ceram. Soc. 84 (10) (2001) 2265–2268.
[18] Mohd Al Amin Muhamad Nor, Lee Chain Hong, Zainal Arifin Ahmad, Hazizan Md Akil, Preparation and characterization of ceramic foam produced via polymeric foam replication method, J. Mater. Process. Technol. 207 (2008) 235–239.
[19] N.R. Cameron, D.C. Sherrington, L. Albiston, D.P. Gregory, Study of the formation of the open-cellular morphology of poly(styrene/divinylbenzene) polyHiPE materials by cryo-SEM, Colloid Polym. Sci. 274 (1996) 592–595.
[20] C. Motz, O. Friedl, R. Pippan, Fatigue crack propagation in cellular metals, Int. J. Fatigue 27 (2005) 1571–1581.
[21] V. Goussery, Y. Bienvenu, S. Forest, A.-F. Gourgues, C. Colin, J.-D. Bartout, Grain size effects on the mechanical behavior of open-cell nickel foams, Adv. Eng. Mater. 6 (6) (2004) 432–439.
[22] S. Soubielle, L. Salvo, F. Diologent, A. Mortensen, Fatigue and cyclic creep of replicated microcellular aluminium, Mater. Sci. Eng. A 528 (2011) 2657–2663.
[23] J. Zhou, W.O. Soboyejo, Compression–compression fatigue of open cell aluminum foams: macro-/micro-mechanisms and the effects of heat treatment, Mater. Sci. Eng. A 369 (2004) 23–35.
[24] Y. Conde, R. Doglione, A. Mortensen, Influence of microstructural heterogeneity on the scaling between flow stress and relative density in microcellular Al–4.5 %Cu, J. Mater. Sci. 49 (2014) 2403–2414.
[25] V. Gergely, B. Clyne, The FORMGRIP process: foaming of reinforced metals by gas release in precursors, Adv. Eng. Mater. 2 (4) (2000) 175–178.
[26] E. Amsterdam, P.R. Onck, T.M. DeHosson, Fracture and microstructure of open cell aluminum foam, J. Mater. Sci. 40 (2005) 5813–5819.
[27] P. Zhang, M. Haag, O. Kraft, A. Wanner, E. Arzt, Microstructural changes in the cell walls of a closed-cell aluminium foam during creep, Philos. Mag. A 82 (16) (2002) 2895–2907.
[28] J.-Y. Buffière, É. Maire, J. Adrien, J.-P. Masse, E. Boller, In situ experiments with X-ray tomography: an attractive tool for experimental mechanics, Exp. Mech. 50 (2010) 289–305.
[29] J. Baruchel, J.-Y. Buffiere, P. Cloetens, M. Dimichiel, E. Ferrie, W. Ludwig, É. Maire, L. Salvo, Advances in synchrotron radiation microtomography, Scr. Mater. 55 (2006) 41–46.
[30] A. Faridani, K.A. Buglione, P. Huabsomboon, O.D. Iancu, J. McGrath, Introduction to local tomography, Contemp. Math. 278 (2001) 29–47.
[31] E.L. Ritman, S.M. Jorgensen, P.E. Lund, P.J. Thomas, J.H. Dunsmuir, J.C. Romero, R.T. Turner, M.E. Bolander, Synchrotron-based micro-CT of in situ biological basic functional units and their integration, Proc. SPIE 3149 (1997) 13–24.
[32] S. Bonnet, F. Peyrin, F. Turjman, R. Prost, Tomographic reconstruction using nonseparable wavelets, IEEE Trans. Image Process. 9 (2000) 1445.

[33] H. Toda, T. Ohgaki, K. Uesugi, K. Makii, Y. Aruga, T. Akahori, M. Niinomi, T. Kobayashi, Quantitative assessment of microstructure and its effects on compression behavior of aluminum foams via high-resolution synchrotron X-ray tomography, Key Eng. Mater. 297–300 (2005) 1189.
[34] Yu-chen Karen Chen-Wiegart, Ross DeMike, Can Erdonmez, Katsuyo Thornton, Scott A. Barnett, Jun Wang, Tortuosity characterization of 3D microstructure at nano-scale for energy storage and conversion materials, J. Power Sources 249 (Jun 2014) 349–356.
[35] Y.-C. K. Chen-Wiegart, T. Wada, N. Butakov, X. Xiao, F. De Carlo, H. Kato, J. Wang, D.C. Dunand, É. Maire, 3D morphological evolution of porous titanium by X-ray micro- and nano-tomography, J. Mater. Res. 28 (2013) 2444–2452.
[36] Karen Chen-Wiegart, Zhao Liu, Katherine T. Faber, Scott A. Barnett, Jun Wang, 3D analysis of a $LiCoO_2$–$Li(Ni_{1/3}Mn_{1/3}Co_{1/3})O_2$ Li-ion battery positive electrode using x-ray nano-tomography, Electrochem. Commun. 28 (Jun 2013) 127–130.
[37] J.W. Bullard, E.J. Garboczi, W.C. Carter, E.R. Fuller, Numerical methods for computing interfacial mean curvature, Comput. Mater. Sci. 4 (1995) 103–116.
[38] F. Flin, J.-B. Brzoska, B. Lesaffre, C. Coléou, R.A. Pieritz, Three-dimensional geometric measurements of snow microstructural evolution under isothermal conditions, Ann. Glaciol. 38 (2004) 39–44.
[39] D. Bauer, S. Youssef, M. Fleury, S. Bekri, E. Rosenberg, O. Vizika, Improving the estimations of petrophysical transport behavior of carbonate rocks using a dual pore network approach combined with computed microtomography, Transp. Porous Media 94 (2012) 505–524.
[40] N. Babcsán, D. Leitlmeier, H.P. Degischer, J. Banhart, The role of oxidation in blowing particle-stabilised aluminium foams, Adv. Eng. Mater. 6 (6) (2004) 421–428.
[41] F. Garcia-Moreno, M. Mukherjee, C. Jiménez, A. Rack, J. Banhart, Metal foaming investigated by X-ray radioscopy, Metals 2 (2012) 10–21.
[42] S. Deville, É. Maire, G. Bernard-Granger, A. Lasalle, A. Bogner, C. Gauthier, J. Leloup, C. Guizard, Metastable and unstable cellular solidification of colloidal suspensions, Nat. Mater. 8 (2009) 966–972.